Eur J Nucl Med Mol Imaging (2014) 41:1046–1056
DOI 10.1007/s00259-014-2691-0

ORIGINAL ARTICLE

Prognostic value of ^{18}F-DOPA PET/CT at the time of recurrence in patients affected by neuroblastoma

Arnoldo Piccardo · Matteo Puntoni · Egesta Lopci · Massimo Conte · Luca Foppiani · Stefania Sorrentino · Giovanni Morana · Mehrdad Naseri · Angelina Cistaro · Giampiero Villavecchia · Stefano Fanti · Alberto Garaventa

Received: 24 October 2013 / Accepted: 2 January 2014 / Published online: 22 February 2014

Abstract
Purpose The aim of this study was to investigate the relationship between ^{123}I-metaiodobenzylguanidine (MIBG) scan semi-quantification and a new ^{18}F-DOPA positron emission tomography (PET)/CT score in patients with suspected or documented neuroblastoma (NB) relapse and to assess the association between these two parameters and progression-free survival (PFS)/overall survival (OS).
Methods We analysed 24 NB patients who had undergone ^{123}I-MIBG and ^{18}F-DOPA PET/CT scans at the time of suspected relapse, after applying a proper scoring system for each scan. In time-to-event analyses, the score distributions were regarded as continuous and were categorized in tertiles and medians. We used Kaplan-Meier curves and Cox proportional hazard models for PFS and OS in order to estimate the independent prognostic impact of ^{123}I-MIBG and ^{18}F-DOPA PET/CT scans.
Results The ^{123}I-MIBG and ^{18}F-DOPA scores were highly and positively correlated (Spearman's rho=0.8, $p<0.001$). Over a median follow-up of 14 months (range 6–82), 12 cases of disease progression and 6 deaths occurred. Multivariate Cox models showed a higher risk of disease progression [hazard ratio (HR) 17.0, 95 % confidence interval (CI) 2.7–109] in NB patients with ^{123}I-MIBG score>3 (3rd tertile) and an even higher risk (HR:37.2, 95 % CI 2.4–574) in those with ^{18}F-DOPA whole-body metabolic burden (WBMB) >7.5 (median), after adjustment for all main clinical/pathological factors considered. Kaplan-Meier analyses showed a significant association with OS (log-rank $p=0.01$ and $p=0.03$ for ^{123}I-MIBG and ^{18}F-DOPA WBMB, respectively).
Conclusion Our results confirm the good agreement between ^{18}F-DOPA PET/CT and ^{123}I-MIBG scan in patients affected by NB relapse. In time-to-event analyses, ^{123}I-MIBG scan and ^{18}F-DOPA PET/CT scores were independently and significantly associated with disease progression.

Keywords Neuroblastoma · ^{123}I-MIBG score · ^{18}F-DOPA PET · Prognostic value

Stefano Fanti and Alberto Garaventa share senior co-authorship.

A. Piccardo · M. Naseri · G. Villavecchia
Nuclear Medicine Unit, Galliera Hospital, Genoa, Italy

M. Puntoni
Clinical Trial Research Unit, Galliera Hospital, Genoa, Italy

E. Lopci · S. Fanti
Nuclear Medicine Unit, Sant'Orsola-Malpighi Hospital, Bologna, Italy

M. Conte · S. Sorrentino · A. Garaventa
Department of Hematology-Oncology, G. Gaslini Children's Hospital, Genoa, Italy

L. Foppiani
Internal Medicine, Galliera Hospital, Genoa, Italy

G. Morana
Department of Pathology and Radiology, G. Gaslini Children's Hospital, Genoa, Italy

A. Cistaro
PET Centre, IRMET, Turin, Italy

A. Piccardo (✉)
Department of Nuclear Medicine, E.O. Ospedali Galliera, Mura delle Cappuccine 14, 16128 Genoa, Italy
e-mail: arnoldo.piccardo@galliera.it

Introduction

As more than 50 % of patients affected by high-risk neuroblastoma (NB) may relapse after initial treatment [1], the long-term cure rate is low, ranging from 25 to 30 % [2, 3]. The principal prognostic factors for post-relapse survival, which have recently been investigated, are age, stage, *MYCN* status

and the length of time (from diagnosis) to first relapse (TTFR) [4]. However, little can be said about the prognostic role of the imaging performed at the time of first recurrence. ^{123}I-Metaiodobenzylguanidine (MIBG) scintigraphy is the technique of choice for NB and has high diagnostic accuracy both in staging at the time of the first diagnosis and in restaging at the time of relapse. Moreover, ^{123}I-MIBG has proved to be a sensitive and specific biomarker in the detection of NB and treatment response evaluation [5], and the persistence of disease documented by ^{123}I-MIBG scan after induction therapy is considered an unfavourable prognostic factor [6, 7]. In particular, when considering ^{123}I-MIBG scan semi-quantification in high-risk NB, patients with scores >3 following induction treatment are reported to have significantly worse event-free survival (EFS) than those with ^{123}I-MIBG scores ≤3 [6]. However, few data are available on the prognostic significance of ^{123}I-MIBG scan at the time of relapse, and the results reported show no significant association between ^{123}I-MIBG imaging findings (skeletal scoring system and soft tissue localization) and survival [overall survival (OS) and progression-free survival (PFS)] [8, 9].

^{18}F-DOPA positron emission tomography (PET)/CT, a valuable diagnostic tool capable of identifying tumours with elevated catecholamine metabolism, has recently been demonstrated to be able to detect NB relapse with high accuracy [10–12]. When directly compared with ^{123}I-MIBG scan, ^{18}F-DOPA PET/CT has been reported to display significantly higher sensitivity [10, 12]. ^{18}F-DOPA PET/CT seems to be more accurate than ^{123}I-MIBG scan in detecting small MIBG-negative metastases, both in soft tissue lesions and in bone marrow localizations. From a practical point of view, the use of ^{18}F-DOPA PET is related to a relatively low acquisition time (12–15 min) just 50 min after injection. By contrast, the dose exposure of ^{18}F-DOPA PET is higher than that of ^{123}I-MIBG [13, 14]. However, no data regarding the prognostic value of ^{18}F-DOPA PET/CT performed at the time of NB recurrence are as yet available.

The aim of this study was to test the relationship between the ^{123}I-MIBG scan scoring system and a new system of ^{18}F-DOPA PET/CT semi-quantification in patients with suspected or documented NB relapse. In addition, we evaluated the association between these two parameters and PFS and OS.

Materials and methods

We retrospectively evaluated a total of 24 consecutive NB patients who had undergone ^{123}I-MIBG scintigraphy and ^{18}F-DOPA PET/CT at the time of suspected or documented relapse on routine clinical and conventional radiological imaging (CT and/or MRI) during follow-up. The main characteristics of patients and tumours are summarized in Table 1. The Local Ethics Committee approved the study.

Imaging modality

All patients with suspected recurrence of disease had a ^{123}I-MIBG-positive scan at the time of the first NB diagnosis. On restaging, ^{123}I-MIBG scintigraphy and ^{18}F-DOPA PET/CT were performed on fasting patients within 10 days of each other; no treatment was administered between the two scans. Image acquisition was performed according to standard procedures. ^{123}I-MIBG scans were acquired 24 h after injection of the tracer by means of a dual-head gamma camera (Millennium, GE Medical Systems, Milwaukee, WI, USA). The activity administered was calculated according to the patient's body weight, with a minimum activity of 80 MBq as suggested by Lassmann et al. [16]. Single photon emission computed tomography (SPECT) images were acquired at intervals of 24 h, if deemed necessary for anatomical localization of the lesion or clarification of equivocal findings as suggested by Matthay et al. [17].

The scan speed for whole-body imaging was 5 cm/min. The dual-head gamma scintillation camera was equipped with a low-energy high-resolution parallel-hole collimator. For SPECT acquisitions, the following parameters were used: 64 projections, 128×128 matrix and 40 s acquisition time per projection. SPECT data were reconstructed by means of an iterative reconstruction algorithm, using a Butterworth filter [17, 18]. Attenuation correction and motion correction software were not available.

Whole-body ^{18}F-DOPA PET/CT was carried out 60 min after the injection of tracer; data were acquired in two-dimensional mode by means of a dedicated PET/CT system (Discovery ST, GE Medical Systems, Milwaukee, WI, USA). The activity administered was calculated according to the patient's body weight (4 MBq/kg), with a minimum activity of 80 MBq. Whole-body ^{18}F-DOPA PET acquisitions were carried out in six to ten bed positions (4-min emissions per bed position) and were reconstructed by using an iterative reconstruction algorithm. No carbidopa premedication was utilized for any PET/CT scans. ^{18}F-DOPA (IASOdopa®) was produced as previously described [19]. A non-diagnostic CT scan (low-dose CT with 120 kV, 80 mA, 0.6 s per rotation) was used for attenuation correction and for anatomical localization of the hot spots of the ^{18}F-DOPA PET study. Motion correction software was not available.

Scoring systems

The effectiveness of ^{123}I-MIBG and ^{18}F-DOPA PET/CT in detecting NB was assessed by reviewing the uptake patterns for each radiopharmaceutical in the following locations: residual tumour, local and regional soft tissue recurrence/metastases, and bone and bone marrow metastases. A semi-quantitative scoring system for NB, the SIOPEN method 3 scoring system, was applied to the ^{123}I-MIBG scan in order to

Table 1 Patient/tumour characteristics and therapeutic strategy at the time of ^{18}F-DOPA PET/CT and ^{123}I-MIBG scintigraphy

Patients	Sex	Age[a] (years)	Stage of disease INNS	*MYCN* gene amplification (yes/no)	TTFR	Sites of primary tumour	Surgery for primary tumour (yes/no)	Systemic therapy (yes/no)	Therapeutic ^{131}I-MIBG (yes/no)	Bone marrow transplantation (yes/no)
1	M	4	4	N	2	Thorax	Y	NB AR 01	N	N
2	M	9	4S	N	9	Abdomen	Y	N	N	N
3	M	8	4	Doubtful	2	Abdomen	Y	NB AR 01	N	N
4	M	6	4	Y	2	Abdomen	Y	NB AR 01+TVD	N	N
5	F	9	4	N	5	Thorax	N	NB unresectable	N	N
6	M	13	4	Y	9	Abdomen	N	NB unresectable	Y	Y
7	M	11	1	N	1	Abdomen	Y	N	N	N
8	F	9	3	N	7	Abdomen	Y (partial)	NB unresectable	N	N
9	F	19	3	N	1	Abdomen	Y	NB AR 01	N	N
10	F	20	3	N	1	Neck	N	NB AR 01	N	N
11	M	5	4	Y	2	Neck	Y	NB unresectable	N	Y
12	F	3	4	N	2	Abdomen	N	NB AR 01	Y	Y
13	M	7	4	N	3	Abdomen	Y	NB AR 01	N	Y
14	M	18	4	N	12	Abdomen	N	AIEOP 92	Y	Y
15	F	8	3	N	1	Abdomen	Y	N	N	N
16	M	41	4	N	3	Abdomen	Y	Y	N	N
17	M	30	4	Not available	7	Abdomen	Y	Y	N	N
18	M	8	2B	Y	5	Abdomen	Y	LNESG2	N	Y
19	M	21	2	Not available	19	Abdomen	Y (partial)	Y	Y	N
20	M	19	4	Y	15	Neck	N	NB 97	N	Y
21	M	2	4	Y	1	Abdomen	Y	NB AR 01	N	N
22	M	4	4	Y	1	Abdomen	Y	NB AR 01	N	N
23	M	8	3	N	1	Thorax	N	NBL 99.1	N	N
24	M	3	4	Y	1	Abdomen	Y	NB AR 01	N	N

NB AR 01: chemotherapy protocol; NB 97: chemotherapy protocol; NBL 99.1: chemotherapy protocol; LNESG2: chemotherapy protocol; AIEOP 92: chemotherapy protocol; TVD (topotecan, vincristine, doxorubicin): chemotherapy protocol

INSS International Neuroblastoma Staging System [15]

[a] Age at the time of suspected relapse

evaluate disease extent in the bone and bone marrow (bone and bone marrow ^{123}I-MIBG score) [6]. The skeletal distribution of ^{123}I-MIBG was recorded in 12 anatomical body segments as follows: skull, thoracic cage, proximal right upper limb, distal right upper limb, proximal left upper limb, distal left upper limb, spine, pelvis, proximal right lower limb, distal right lower limb, proximal left lower limb and distal left lower limb. The extent of skeletal involvement for each bone segment was scored using a 0–6 scale to discriminate between focal lesions and diffuse infiltration. Each segment is scored as 0, no involvement; 1, one discrete lesion; 2, two discrete lesions; 3, three discrete lesions; 4, >3 discrete foci or a single diffuse lesion involving <50 % of a bone; 5, diffuse involvement of >50 to 95 % whole bone; 6, diffuse involvement of the entire bone [6].

To semi-quantify soft tissue NB localization the modified Curie scoring system was applied, based upon the methodology of Matthay et al. (soft tissue ^{123}I-MIBG score) [7]. Soft tissue lesions were scored as follows: 0, no MIBG involvement; 1, one MIBG-avid soft tissue lesion present; 2, more than one MIBG-avid soft tissue lesion present; and 3, MIBG avidity in a soft tissue lesion that occupied 50 % of the chest or abdomen. The ^{123}I-MIBG whole-body score (WBS) was calculated as the sum of bone and bone marrow ^{123}I-MIBG score plus soft tissue ^{123}I-MIBG score.

For ^{18}F-DOPA PET/CT, we applied the SIOPEN method 3 scoring system to evaluate the extent of bone and bone marrow disease. To better characterize the intrinsic metabolic burden of each bone segment (B-MB), we multiplied the mean standardized uptake value (SUV_{mean}) by the score of each bone segment. The whole-body bone metabolic burden (WB-B-MB) was calculated as the sum of the B-MB of each bone segment in the PET image. To determine the extent and the load of soft tissue recurrence/metastases, a whole-body

soft tissue metabolic burden (WB-S-MB) per patient was applied [20]. For each tumour lesion, the soft tissue metabolic burden (S-MB) was calculated as:

$$S{-}MB = SUV_{mean} \times \text{tumour volume}.$$

Tumour volume was obtained from the CT images of the PET/CT acquisitions [21]. The WB-S-MB was calculated as the sum of the MB of each tumour lesion in the PET image. Finally, the overall whole-body metabolic burden (WBMB) was calculated as the sum of WB-B-MB+WB-S-MB.

^{18}F-DOPA PET/CT and ^{123}I-MIBG scan images were interpreted after a consensus reading by two nuclear medicine physicians, who were aware of the patient's clinical history but blinded to any results of the anatomical imaging modalities (MRI/CT).

Standards of reference

The standard of reference for primary residual tumour and locoregional soft tissue recurrence/metastases was based on histopathology (available in 8 of 24 patients) and/or diagnostic contrast-enhanced CT and/or MRI findings (available in all patients).

The gold standards for bone and bone marrow metastases were bone marrow biopsy (available in 19 of 24 patients), CT and/or MRI (available in all patients). A median clinical and imaging follow-up time of 14 months (range 6–82) was available for each patient.

Statistical methods

Descriptive statistics included mean, standard deviation, median, percentiles, minimum and maximum of continuous factors and scores; in the case of categorical factors, number and percentage distribution were used. Pearson's chi-square and Kruskal-Wallis or Mann-Whitney U tests were used to compare categorical and continuous factors, respectively.

Spearman's rank correlation coefficient was used to test the correlation between ^{123}I-MIBG WBS and ^{18}F-DOPA WBMB; positive predictive value (PPV) and negative predictive value (NPV) were used for descriptive purposes.

Kaplan-Meier estimates of the cumulative probability of PFS and OS—defined as the interval between initial diagnosis and the onset of disease progression and as death from any cause, respectively—were obtained. The Cox proportional hazard model was used to estimate the risk of disease progression and death from any cause, after adjustment for age, sex, age on recurrence and bone/bone marrow involvement. The proportional hazard assumption was graphically checked. ^{123}I-MIBG WBS and ^{18}F-DOPA WBMB were highly correlated; thus, to avoid collinearity, we used different models for each score to test their independent association with PFS and OS. Each score was first tested as a continuous variable in the model, then as a binary variable considering the 3rd tertile (=3) for ^{123}I-MIBG score and the median (=7.5) for ^{18}F-DOPA WBMB as cut-off points. To make the results more readable to clinicians, they are mainly presented in relation to these cut-off points. Moreover, a MIBG cut-off value of 3 could have clinical significance, considering that a score >3 after induction therapy has previously been regarded as a prognostic factor able to identify patients more likely to suffer relapse [6, 7]

All analyses were conducted by means of Stata (version 11, StataCorp., College Station, TX, USA) software. Two-tailed probabilities are reported and a p value of 0.05 was used to define nominal statistical significance.

Results

^{18}F-DOPA PET/CT identified disease recurrence in 17 of the 24 patients, while ^{123}I-MIBG scan was positive in 16. Combined analysis of ^{18}F-DOPA PET/CT and ^{123}I-MIBG scan for each patient revealed recurrence in 18 of the 24 patients. Our multidisciplinary diagnosis and clinical and imaging follow-up confirmed disease recurrence in all 18. The absence of disease relapse was confirmed in the other six patients. The PPV and NPV of ^{18}F-DOPA PET/CT were 100 and 86 %, respectively. The PPV and NPV of ^{123}I-MIBG scans were 100 and 75 %, respectively. Disease progression was observed in 12 of 18 patients affected by NB recurrence. No patients with negative ^{18}F-DOPA PET/CT and negative ^{123}I-MIBG scan developed disease progression. One patient with negative ^{18}F-DOPA PET/CT and positive ^{123}I-MIBG scan developed disease progression. Two patients with positive ^{18}F-DOPA PET/CT and negative ^{123}I-MIBG scan developed disease progression. Of 12 patients with disease progression, 6 died of disease (DOD) (Table 2).

^{123}I-MIBG WB and ^{18}F-DOPA WBMB scores were highly and positively correlated (Fig. 1). However, ^{18}F-DOPA WBMB showed greater dispersion than ^{123}I-MIBG WBS, displaying an interquartile range from 0 to 15.0 versus 0 to 4.5 for ^{123}I-MIBG (Fig. 2). Representative images of two matching scans are shown in Fig. 3.

After a median clinical and imaging follow-up time of 14 months (range 6–82), patients with ^{123}I-MIBG WBS >3 had a significantly higher risk of disease progression (log-rank p= 0.001) and death (p=0.01) than those with ^{123}I-MIBG WBS ≤3 (Fig. 4). As regards DOPA score, on considering quartiles of distributions, Kaplan-Meier curves clearly defined a gradient of risk for disease progression, starting from the lowest risk for patients with DOPA score <1 (1st quartile) to the highest risk for patients with ^{18}F-DOPA WBMB>15 (4th quartile) (log-rank p=0.0004) (Fig. 5). Patients with a ^{18}F-DOPA WBMB >7.5 (median) displayed a significantly higher

Table 2 Results of imaging studies and outcome of 24 NB patients

Patients	DOPA PET/CT results	MIBG scan results	SPECT acquisition (yes/no)	DOPA WBMB	MIBG WBS	Bone marrow involvement (yes/no)	Disease progression (yes/no)	Dead of disease (yes/no)
1	Positive	Positive	N	51	43	Y	Y	Y
2	Positive	Positive	N	37	1	N	Y	Y
3	Positive	Negative	N	10	0	N	Y	N
4	Positive	Positive	Y	10	8	Y	Y	N
5	Positive	Positive	Y	11	5	Y	Y	Y
6	Positive	Positive	N	51	39	Y	Y	Y
7	Positive	Positive	Y	12	4	Y	N	N
8	Positive	Positive	Y	8	1	N	N	N
9	Positive	Negative	Y	1	0	N	Y	N
10	Negative	Negative	Y	0	0	N	N	N
11	Positive	Positive	Y	18	6	Y	Y	N
12	Positive	Positive	Y	6	2	N	N	N
13	Negative	Negative	Y	0	0	N	N	N
14	Negative	Negative	Y	0	0	N	N	N
15	Positive	Positive	Y	3	1	N	N	N
16	Positive	Positive	Y	15	4	N	Y	N
17	Positive	Positive	Y	17	1	N	Y	N
18	Negative	Negative	Y	0	0	N	N	N
19	Positive	Positive	Y	8	1	N	N	N
20	Negative	Negative	Y	0	0	N	N	N
21	Positive	Positive	Y	15	8	Y	Y	Y
22	Negative	Positive	Y	0	1	N	Y	Y
23	Negative	Negative	Y	0	0	N	N	N
24	Positive	Positive	Y	5	3	Y	N	N

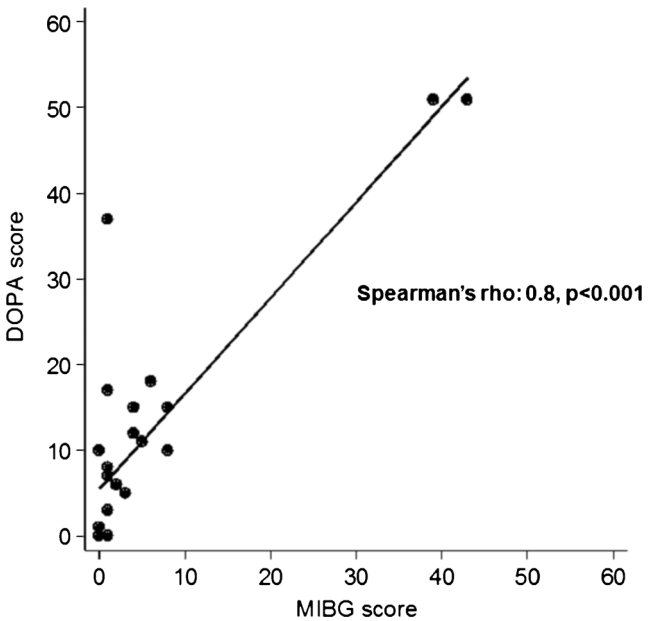

Fig. 1 ^{18}F-DOPA WBMB and ^{123}I-MIBG WBS; a significant positive correlation between these two parameters was found

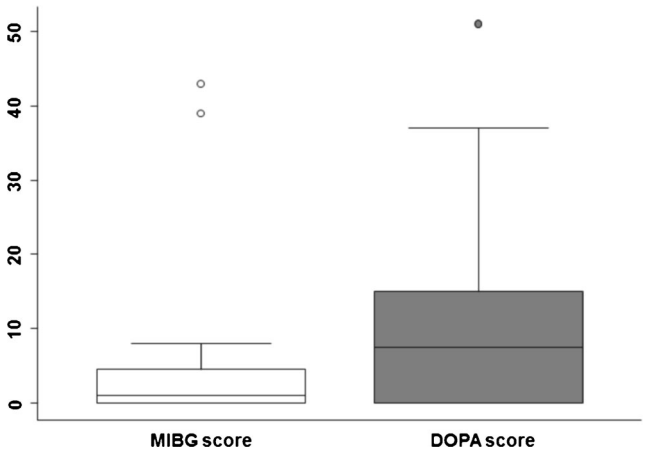

Fig. 2 Box plots of ^{18}F-DOPA WBMB and ^{123}I-MIBG WBS distributions: the *bottom* and *top* of the boxes are the 1st and 3rd quartiles, and the *band* inside the box is the median (2nd quartile); the *whiskers* represent the lowest value still within 1.5 interquartile range (IQR) of the lower quartile, and the highest value still within 1.5 IQR of the upper quartile; the *small circles* represent two outliers for MIBG score (patients 1 and 6) and one outlier for DOPA score (patient 1). The inter-patient variability of ^{18}F-DOPA scores proved higher than that of the ^{123}I-MIBG scan scoring system

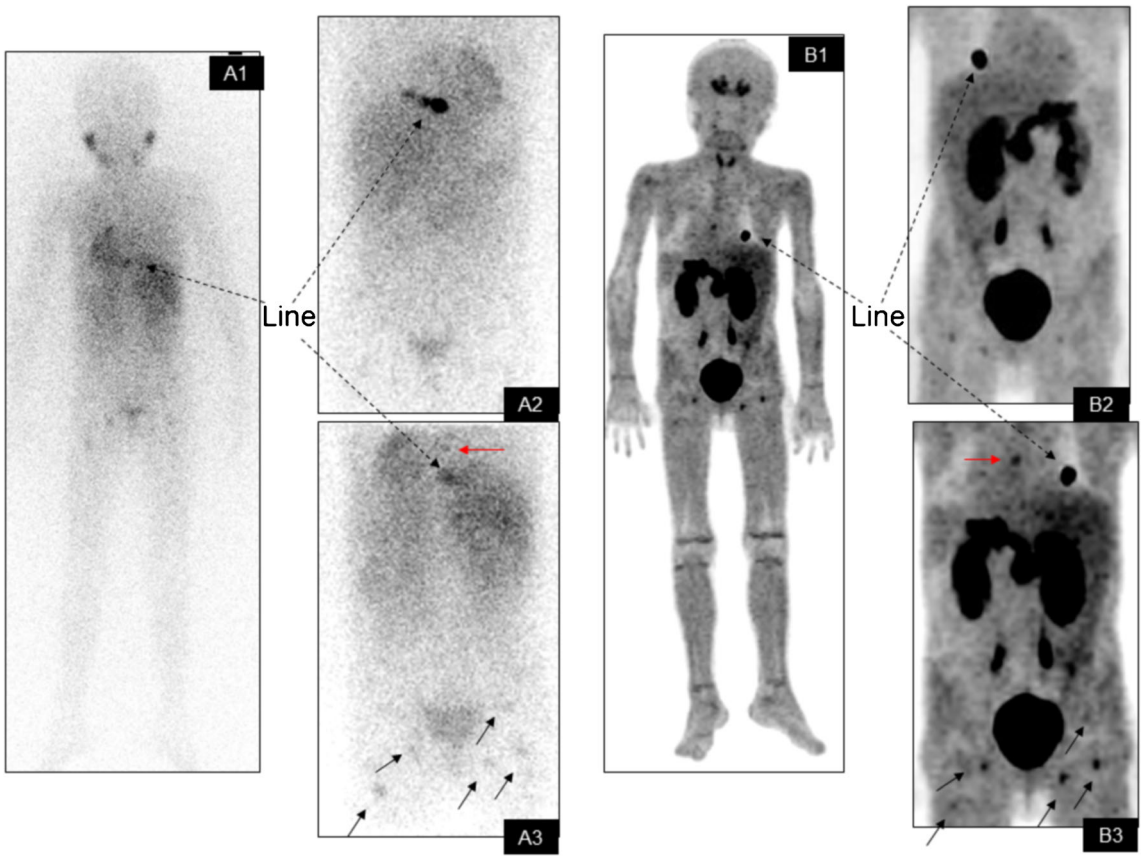

Fig. 3 A 6-year-old child affected by bone and bone marrow NB recurrence (patient 4). Whole-body ^{123}I-MIBG scan (posterior view *A1*) with additional spot images of the chest and abdomen (anterior and posterior views *A2* and *A3*) and ^{18}F-DOPA PET MIP (anterior and posterior views *B1*, *B2* and *B3*) detected the same number of bone/bone marrow metastases; one was detected in the spine (*red arrow*) and five in the pelvis (*black arrows*). The injection site is marked by *dashed arrows*

risk of death from any cause (log-rank p=0.037) than those with ^{18}F-DOPA WBMB≤7.5 (Fig. 6).

Risk estimates (unadjusted and adjusted) for disease progression were calculated from the Cox model (Table 3). After adjustment for age/age at disease onset/at recurrence, sex, bone/bone marrow involvement and time from disease onset to recurrence, the risk of disease progression remained significantly higher for patients with ^{123}I-MIBG WBS >3 than for those with ^{123}I-MIBG WBS ≤3 [hazard ratio (HR) 17.0, 95 % confidence interval (CI) 2.7–109, p=0.003] (Table 3). Similarly, NB patients with ^{18}F-DOPA WBMB>7.5 had a higher risk of disease progression than those with ^{18}F-DOPA WBMB≤7.5 (HR 37.2, 95 % CI 2.4–574) (Table 3). On considering MIBG and DOPA scores as continuous variables in the multivariate models, it was estimated that a 1-unit increase in MIBG score corresponded to a mean increase of 44 % in the risk of disease progression (HR per 1-unit score increase 1.44, 95 % CI 1.03–2.00, p=0.03) and that a 1-unit increase in DOPA score corresponded to a 24 % increase (HR per 1-unit score increase 1.24, 95 % CI 1.08–1.41, p=0.002) (Table 4).

The only other factor independently and directly associated with disease progression was stage at disease onset (Table 3). A trend towards a direct association between TTFR and disease progression was also found, though the risk estimates were not statistically significant. Cox modelling was not applicable to OS analysis, owing to the lack of statistical power (few events).

Discussion

To date, no data are available on the prognostic role of ^{18}F-DOPA PET/CT in NB patients at the time of recurrence. Moreover, little can be said about the prognostic significance of ^{123}I-MIBG scan at the time of relapse, since the results reported in the literature have shown no significant association between ^{123}I-MIBG imaging findings and survival [8, 9]. Indeed, the ^{123}I-MIBG scoring system has not been assessed by important retrospective analyses, such as the recent study by London et al. [4], which investigated the principal prognostic factors at the time of NB recurrence. We therefore tried to address this issue by comparing these two imaging modalities with respect to disease prognostication and patient outcome.

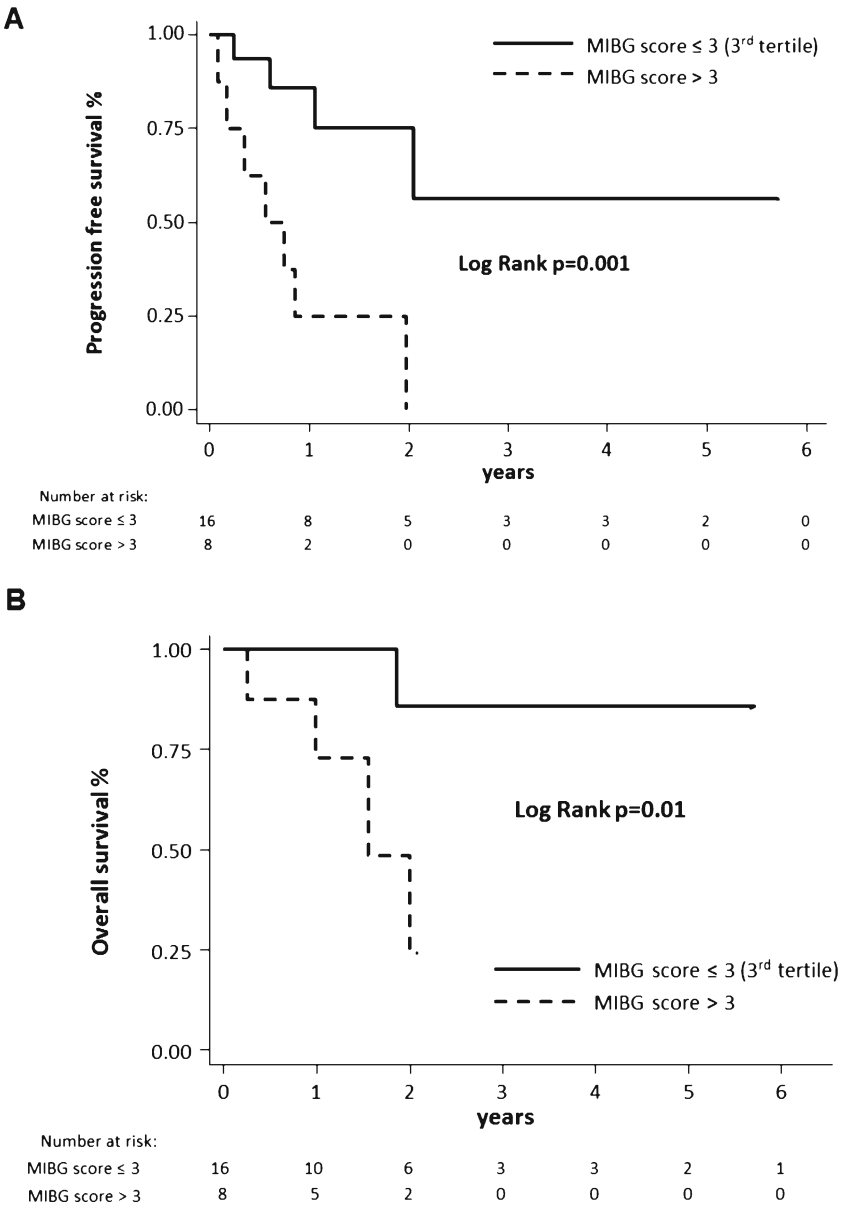

Fig. 4 Kaplan-Meier PFS curves (**a**) and OS curves (**b**) according to ^{123}I-MIBG WBS≤3 and>3 (3rd tertile)

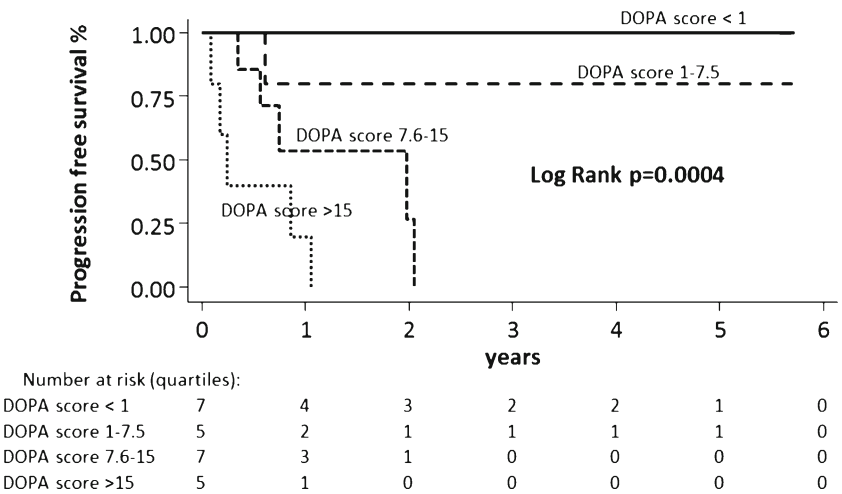

Fig. 5 Kaplan-Meier PFS curves according to ^{18}F-DOPA WBMB quartiles (<1, 1–7.5, 7.6–15 and >15)

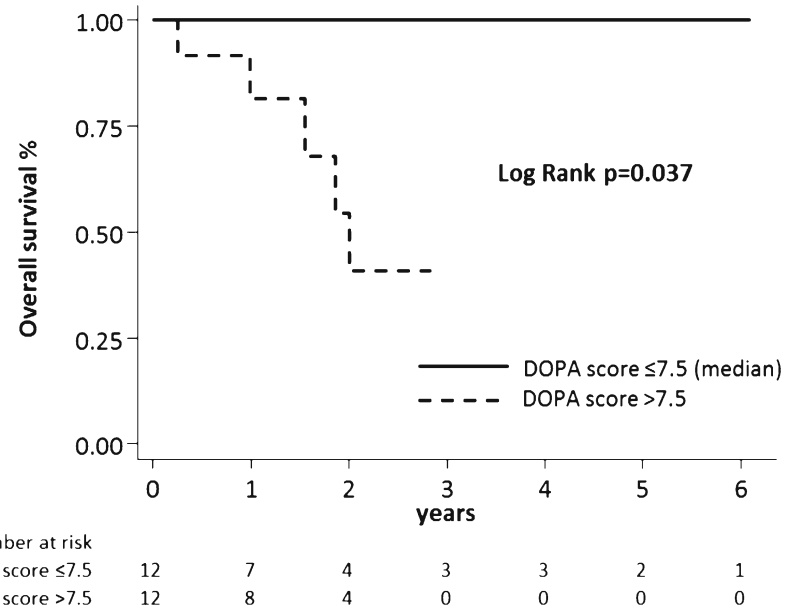

Fig. 6 Kaplan-Meier OS curves according to ^{18}F-DOPA WBMB ≤7.5 and>7.5 (median)

Our study confirmed the high accuracy of ^{18}F-DOPA PET/CT and ^{123}I-MIBG scanning in the assessment of NB at the time of suspected relapse on routine clinical and conventional radiological imaging during follow-up [11, 22, 23]. In particular, the PPV of ^{18}F-DOPA PET/CT and ^{123}I-MIBG scan for NB recurrence was 100 %.

Moreover, to our knowledge, the present study is the first to determine the predictive role of ^{18}F-DOPA PET/CT at the time of suspected NB relapse. Our data were gathered over a long-term follow-up of each patient (median 14 months) and relate to both disease progression and death. Indeed, 12 of the 18 patients affected by NB recurrence developed disease progression, 6 of whom DOD. The relatively low rate of rapid and fatal progression observed may be related to the characteristics of our population; the fact that our study included five adolescents and two adults, who often display longer survival [24], might have impacted on the number of DOD at the end of follow-up.

We also analysed the relationship between ^{123}I-MIBG scan and ^{18}F-DOPA PET/CT semi-quantification and found a significant positive correlation between these two parameters. These findings better express the good agreement between ^{18}F-DOPA PET/CT and ^{123}I-MIBG scans that has previously been postulated [10]. Indeed, in all but one ^{123}I-MIBG-

Table 3 Cox regression analysis of PFS (subjects n=24, events n=12)

Marker	Type of analysis	Variable	HR[a]	95% CI	p
MIBG	Univariate	MIBG WBS ≤3	1.00		
		MIBG WBS >3 (3rd tertile)	6.93	1.77–27.04	0.005
	Multivariate	MIBG WBS ≤3	1.00		
		MIBG WBS >3 (3rd tertile)	17.0	2.66–108.8	0.003
		Stage at disease onset (>3 vs ≤3)	19.7	1.00–385	0.05
		Time from disease onset to recurrence (>2 years vs ≤2 years)	6.52	0.51–83.6	0.15
		MYCN amplification	0.27	0.02–4.38	0.35
DOPA	Univariate	DOPA WBMB ≤7.5	1.00		
		DOPA WBMB >7.5 (median)	15.54	1.94–122.5	0.009
	Multivariate	DOPA WBMB ≤7.5	1.00		
		DOPA WBMB >7.5 (median)	37.2	2.41–573.5	0.01
		Stage at disease onset (>3 vs ≤3)	15.4	0.73–325.2	0.08
		Time from disease onset to recurrence (>2 years vs ≤2 years)	2.33	0.17–31.4	0.53
		MYCN amplification	0.26	0.02–4.33	0.35

[a] Adjusted for age, sex, age at recurrence, bone/bone marrow involvement

Table 4 Cox regression analysis

Type of event	Variable	HR[a]	95% CI	*p*
Progression (events=12)	MIBG WBS (univariate)	1.20	1.01–1.44	0.04
	MIBG WBS (multivariate)	1.44	1.03–2.00	0.03
	DOPA WBMB (univariate)	1.22	1.08–1.37	0.001
	DOPA WBMB (multivariate)	1.24	1.08–1.42	0.002
Death (events=6)	DOPA WBMB (univariate)	1.12	1.03–1.22	0.007
	DOPA WBMB (multivariate)	1.17	0.98–1.40	0.09

[a] per 1-unit increase in score. Multivariate Cox HR are adjusted for age, stage at disease onset, age at disease onset, age at disease recurrence, time from disease onset to recurrence, *MYCN* amplification (yes/no)

positive patient (94 %), ^{18}F-DOPA PET/CT was also positive. Similarly, in 15 of 17 ^{18}F-DOPA-positive patients (88 %), the ^{123}I-MIBG scan was also positive.

The ^{18}F-DOPA PET/CT score, called ^{18}F-DOPA WBMB, considers two important variables that are not completely included in the ^{123}I-MIBG WBS: the extent of soft tissue metastases and uptake intensity. Consequently, the inter-patient variability of ^{18}F-DOPA WBMB proved higher than that of the ^{123}I-MIBG scan scoring system. This greater variability in ^{18}F-DOPA WBMB scores may prompt the reclassification of patients with the same ^{123}I-MIBG score. Specifically, in our study the ^{123}I-MIBG WBS was not well able to stratify patients with soft tissue recurrence but no bone marrow involvement. Indeed, we found five patients (patients 2, 8, 15, 17 and 19) with the same ^{123}I-MIBG WBS (1) but with five different positive ^{18}F-DOPA WBMB, raging from 3 to 37. Two of these patients (patients 2 and 17) with the highest ^{18}F-DOPA WBMB (37 and 17, respectively) developed disease progression.

To evaluate the real prognostic impact of ^{18}F-DOPA PET and its ability to stratify patients, we tested the application of this PET scoring system, as previously reported [20], and the association between this parameter and PFS and OS. We also evaluated the association between ^{123}I-MIBG WBS and PFS and OS. Both these imaging scores proved to be related to the outcome of patients with NB recurrence in terms of PFS and OS. The Kaplan-Meier curves showed a significant difference in terms of PFS and OS between patients with different ^{18}F-DOPA WBMB scores and confirmed that ^{123}I-MIBG WBS correlated inversely with the time of progression. Specifically, our Kaplan-Meier OS curves showed that, 24 months after the diagnosis of recurrence, only 54 % (95 % CI 18–81 %) of patients with ^{18}F-DOPA WBMB >7.5 and 49 % (95 % CI 8–82 %) of patients with ^{123}I-MIBG WBS >3 were alive, versus 100 % with ^{18}F-DOPA WBMB ≤7.5 and 86 % (95 % CI 33–98 %) with ^{123}I-MIBG WBS ≤3 (log-rank p=0.037 and 0.01, respectively) (Figs. 3 and 4).

On multivariate analysis, the imaging scores remained the most important factors associated with PFS (Table 3). Specifically, patients with ^{18}F-DOPA WBMB >7.5 had a higher risk of disease progression than those with ^{18}F-DOPA WBMB ≤7.5. Similarly, patients with ^{123}I-MIBG WBS >3 had a higher risk of disease progression than those with ^{123}I-MIBG WBS ≤3, independently of all other factors included in the multivariate model.

Similar results come from an additional model considering MIBG and DOPA scores as continuous variables: it was estimated that a 1-unit increase in MIBG score corresponded to a 44 % mean increase in the risk of disease progression and that a 1-unit increase in DOPA score corresponded to a 24 % increase. The difference between these mean per cent increases in risk is probably due to the different dispersion of the two scores, DOPA scores being clearly more dispersed.

The data reported might suggest that ^{123}I-MIBG scan and ^{18}F-DOPA PET/CT should not only be regarded as sensitive methods of detecting NB recurrence but also as prognostic factors able to predict disease progression. In this regard, ^{18}F-DOPA PET/CT seems to be better related to PFS than ^{123}I-MIBG scan (HR 37 vs HR 17), as its higher score variability is better able to stratify the risk of each patient.

In our multivariate analysis, all the principal prognostic factors able to predict PFS at the time of recurrence (age, stage, *MYCN* amplification and TTFR) were taken into account. The only variable independently associated with PFS proved to be the NB stage at the time of first diagnosis. A trend towards a direct association between TTFR and disease progression was observed, though the risk estimates were not statistically significant. These findings may have been due to the higher prognostic value of staging than of other variables in a multivariate analysis [4]. Moreover, the lack of a significant correlation between the other well-known prognostic factors and the outcome may well have been due to the low number of patients/events included in our study.

This study has some limitations: (1) the low statistical power (low number of patients and events), (2) the retrospective analysis of the data and (3) the fact that the effect of therapy was not considered. However, another important paper that has recently been published [4] on prognostic factors in NB relapsing patients did not directly consider therapy implications, as treatment on relapse is highly inhomogeneous

and clinically tailored [25]. Another limitation concerns the fact that our population included two adults and five adolescents and was therefore not a typical NB population. Although our cohort has a significant variability in age, we did not detect any difference between younger and older patients in the prognostic value of the scores, both in the univariate (data not shown) and in the multivariate analyses (results were age-adjusted but age was not a statistically significant factor).

Finally, we report the lack of SPECT data in 4 of 24 patients as reported in Table 2. Although SPECT was not performed in these four patients, the ^{123}I-MIBG whole-body scan showed no doubtful findings needing a SPECT protocol in three patients. Patients 1 and 6 had clear and diffuse bone/bone marrow involvement and patient 2 was affected by a big liver metastasis characterized by MIBG uptake. Only in one negative MIBG patient (patient 3), affected by a small submandibular lymph node recurrence detected by ^{18}F-DOPA PET/CT, was SPECT not performed. However, in this patient with lymph node recurrence close to physiological uptake of the right submandibular gland, a SPECT image might have improved the sensitivity of the MIBG scan only theoretically.

Conclusion

Our results showed good agreement between ^{18}F-DOPA PET/CT semi-quantification and ^{123}I-MIBG scan in patients affected by NB relapse, in that a significant positive correlation between the two techniques was observed. In time-to-event analyses, ^{123}I-MIBG scan and ^{18}F-DOPA PET/CT scores were independently and significantly associated with disease progression. Further confirmation on a larger and more homogeneous group of patients is required.

Conflicts of interest None.

References

1. Matthay KK, Villablanca JG, Seeger RC, Stram DO, Harris RE, Ramsay NK, et al. Treatment of high-risk neuroblastoma with intensive chemotherapy, radiotherapy, autologous bone marrow transplantation, and 13-cis-retinoic acid. Children's Cancer Group. N Engl J Med 1999;341:1165–73.
2. Pearson AD, Pinkerton CR, Lewis IJ, Imeson J, Ellershaw C, Machin D, et al. High-dose rapid and standard induction chemotherapy for patients aged over 1 year with stage 4 neuroblastoma: a randomised trial. Lancet Oncol 2008;9:247–56.
3. Zage PE, Kletzel M, Murray K, Marcus R, Castleberry R, Zhang Y, et al. Outcomes of the POG 9340/9341/9342 trials for children with high-risk neuroblastoma: a report from the Children's Oncology Group. Pediatr Blood Cancer 2008;51:747–53.
4. London WB, Castel V, Monclair T, Ambros PF, Pearson AD, Cohn SL, et al. Clinical and biologic features predictive of survival after relapse of neuroblastoma: a report from the International Neuroblastoma Risk Group project. J Clin Oncol 2011;29:3286–92.
5. Jacobson AF, Deng H, Lombard J, Lessig HJ, Black RR.123I-metaiodobenzylguanidine scintigraphy for the detection of neuroblastoma and pheochromocytoma: results of a meta-analysis. J Clin Endocrinol Metab 2010;95:2596–606.
6. Lewington V, Bar Sever Z, Giammarile F, Lynch T, McEwan A, Shulkin B, et al. Development of a semi-quantitative I-123 mIBG reporting method in high risk neuroblastoma. J Nucl Med 2009;50:1379.
7. Matthay KK, Edeline V, Lumbroso J, Tanguy ML, Asselain B, Zucker JM, et al. Correlation of early metastatic response by123I-metaiodobenzylguanidine scintigraphy with overall response and event-free survival in stage IV neuroblastoma. J Clin Oncol 2003;21:2486–91.
8. Papathanasiou ND, Gaze MN, Sullivan K, Aldridge M, Waddington W, Almuhaideb A, et al. 18F-FDG PET/CT and 123I-metaiodobenzylguanidine imaging in high-risk neuroblastoma: diagnostic comparison and survival analysis. J Nucl Med 2011;52:519–25.
9. Messina JA, Cheng SC, Franc BL, Charron M, Shulkin B, To B, et al. Evaluation of semi-quantitative scoring system for metaiodobenzylguanidine (mIBG) scans in patients with relapsed neuroblastoma. Pediatr Blood Cancer 2006;47:865–74.
10. Piccardo A, Lopci E, Conte M, Garaventa A, Foppiani L, Altrinetti V, et al. Comparison of (18)F-dopa PET/CT and (123)I-MIBG scintigraphy in stage 3 and 4 neuroblastoma: a pilot study. Eur J Nucl Med Mol Imaging 2012;39:57–61.
11. Lopci E, Piccardo A, Nanni C, Altrinetti V, Garaventa A, Pession A, et al. 18F-DOPA PET/CT in neuroblastoma: comparison of conventional imaging with CT/MR. Clin Nucl Med 2012;37:e73–8.
12. Lu MY, Liu YL, Chang HH, Jou ST, Yang YL, Lin KH, et al. Characterization of neuroblastic tumors using 18F-FDOPA PET. J Nucl Med 2013;54:42–9.
13. ICRP. Radiation dose to patients from radiopharmaceuticals. Addendum 3 to ICRP publication 53. ICRP publication 106. Ann ICRP 2008;38(1–2):1–197.
14. ICRP. Radiation dose to patients from radiopharmaceuticals (addendum 2 to ICRP publication 53). ICRP Publication 80. Ann ICRP 1998;28(3):1–126.
15. Brodeur GM, Pritchard J, Berthold F, Carlsen NL, Castel V, Castelberry RP, et al. Revisions of the international criteria for neuroblastoma diagnosis, staging, and response to treatment. J Clin Oncol 1993;11:1466–77.
16. Lassmann M, Biassoni L, Monsieurs M, Franzius C, Jacobs F, EANM Dosimetry and Paediatrics Committees. The new EANM paediatric dosage card. Eur J Nucl Med Mol Imaging 2007;34:796–8.
17. Matthay KK, Shulkin B, Ladenstein R, Michon J, Giammarile F, Levington V, et al. Criteria for evaluation of disease extent by 123I-metaiodobenzylguanidine scans in neuroblastoma: a report for the International Neuroblastoma Risk Group (INRG) Task Force. Br J Cancer 2010;102:1319–22.
18. Olivier P, Colarinha P, Fettich J, Fischer S, Frökier J, Giammarile F, et al. Guidelines for radioiodinated MIBG scintigraphy in children. Eur J Nucl Med Mol Imaging 2003;30:B45–50.
19. Luxen A, Perlmutter M, Bida GT, Van Moffaert G, Cook JS, Satyamurthy N, et al. Remote, semiautomated production of 6-[18F]fluoro-L-dopa for human studies with PET. Int J Rad Appl Instrum A 1990;41:275–81.
20. Fiebrich HB, Brouwers AH, Kerstens MN, Pijl ME, Kema IP, de Jong JR, et al. 6-[F-18]Fluoro-L-dihydroxyphenylalanine positron emission tomography is superior to conventional imaging with (123)I-metaiodobenzylguanidine scintigraphy, computer tomography, and magnetic resonance imaging in localizing tumors causing catecholamine excess. J Clin Endocrinol Metab 2009;94:3922–30.

21. Berkowitz A, Basu S, Srinivas S, Sankaran S, Schuster S, Alavi A. Determination of whole-body metabolic burden as a quantitative measure of disease activity in lymphoma: a novel approach with fluorodeoxyglucose-PET. Nucl Med Commun 2008;29:521–6.
22. Okuyama C, Ushijima Y, Kubota T, Nakamura T, Kikkawa M, Nishimura T. Utility of follow-up studies using meta-[123 I] iodobenzylguanidine scintigraphy for detecting recurrent neuroblastoma. Nucl Med Commun 2002;23:663–72.
23. Kushner BH, Kramer K, Modak S, Cheung NK. Sensitivity of surveillance studies for detecting asymptomatic and unsuspected relapse of high-risk neuroblastoma. J Clin Oncol 2009;27:1041–6.
24. Conte M, Parodi S, De Bernardi B, Milanaccio C, Mazzocco K, Angelini P, et al. Neuroblastoma in adolescents: the Italian experience. Cancer 2006;106:1409–17.
25. Morgenstern DA, Baruchel S, Irwin MS. Current and future strategies for relapsed neuroblastoma: challenges on the road to precision therapy. J Pediatr Hematol Oncol 2013;35:337–47.